

# Further Exploration of the Micro Resistive Well

Jacquelyne Miksanek

May 3rd, 2019

## Contents

<b>1</b>	<b>Introduction</b>	<b>2</b>
<b>2</b>	<b>Background</b>	<b>2</b>
<b>3</b>	<b>Gas Leak Testing</b>	<b>3</b>
3.1	Input vs Output Flow Test . . . . .	3
3.2	Quality Control Test Three . . . . .	3
3.3	Using the Leak Hunter . . . . .	3
<b>4</b>	<b>Noise Reduction Testing</b>	<b>4</b>
4.1	Quality Control Test Four . . . . .	4
<b>5</b>	<b>Current-Voltage Curves</b>	<b>4</b>
<b>6</b>	<b>Preamplifier Testing</b>	<b>6</b>
<b>7</b>	<b>Conclusion and Future Work</b>	<b>6</b>

# 1 Introduction

The Micro-Resistive Well ( $\mu$ R-well) is a type of Micro-Pattern Gas Detectors (MPGD) and is currently in research and development as a candidate for the future Electron Ion Collider (EIC). This particular MPGD is suitable for large area tracking and operation in harsh radiation environments. Unlike other MPGDs, the  $\mu$ R-well has a single amplification stage and a micro-patterned well design constructed from a polyimide foil and a diamond-like-carbon (DLC) resistive layer. The structure of the detector can be seen in Figure 1 where the detector begins with a drift cathode followed by a drift gap of 3mm. The wells, DLC, and readout electronics are formed on a sturdy honeycomb structured board.

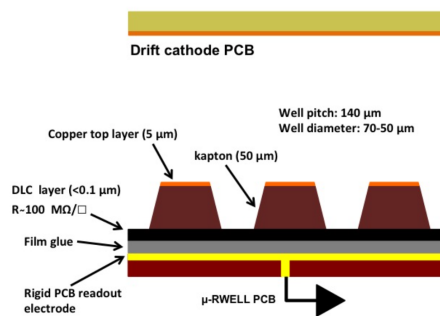


Figure 1: A cross-section of the cathode and readout structure. Charges that are amplified in the wells are collected on the DLC layer and an induced signal is seen on the readout electrode that is then sent to external readout electronics for processing.

# 2 Background

The  $\mu$ R-well was designed to limit harmful sparking that occurs in other MPGDs, such as the Gas Electron Multiplier (GEM). Sparking occurs when a new path is forged by a particle of dust, or anything that has a resistivity. A high voltage will allow current to pass through the new path creating an electrical short from a spontaneous discharge. Overtime, sparking will cause irreparable damage to the detectors. The added DLC resistive layer helps to mitigate the sparking by allowing pent up electrical charge to disperse along the powerful resistive layer.

When a charged particle enters the detector a preliminary ionization is produced through collisions that ionize  $ArCO_2$  gas molecules. A secondary ionization occurs in the detector's single amplification stage through an electron avalanche, where an electric field produced by a potential difference across the well structure acts as a catalyst for the process. The charge is then collected on the resistive DLC layer, and an induced signal is seen on the readout.

## 3 Gas Leak Testing

### 3.1 Input vs Output Flow Test

Two large flow meters were used to monitor input and output gas flow for the  $\mu$ R-well. Helium gas was input at a flow of 30 units on the large flow meter which resulted with an output flow with approximately a 40% gas loss. The test was repeated with an input flow of 40 units on the large flow meter and once again an approximate 40% gas loss was seen in the output flow meter. A gas leak was determined to be present.

### 3.2 Quality Control Test Three

Quality control test three is used to ensure the chamber of the detector is gas tight. This is done by filling the chamber with Helium gas until a 5 millibar pressure is reached. The chamber is then closed off and the pressure is monitored over a period of three hours. Ideally, the pressure should be unchanged over this amount of time which would indicate a gas tight detector. The  $\mu$ R-well was proven to have a small gas leak over the course of testing. All pressure was lost in the chamber within 10 seconds after closing the lines. Further testing with leak hunters was completed to investigate the source of the leak. Possible sources include a non-uniform o-ring, and non-uniformly tightened closing screws. Some closing screws were noticed to be stripped and could be tightened at the same rate surrounding screws were, after a torque was applied. The more likely source of the gas leak is a non-uniform o-ring or the groove depth of the frame. Due to the scale that the detector functions on, even a small change in diameter of the o-ring, such as a fraction of a millimeter, could vastly compromise the seal of the detector. If the groove depth is too deep or too shallow it could create gaps allowing gas to leak through. This has also been a problem with past detectors, specifically the GE1/1 detectors.

### 3.3 Using the Leak Hunter

An attempt to find the source of the leak was done using a leak hunter (model number 8066) and Helium gas. This leak hunter functions by detecting specific gases in the atmosphere like Helium, by measuring the conductivity. If Helium gas was found to be present near the sensor the leak hunter it would notify the user that there is a possible leak at that location. The results from this ruled out a possible leak around the window of the detector, the outer frame of the detector was flagged by the leak hunter to be a possible source of the leak. It was, however, not accurate with locating a specific source region for the leak. A PlantScan ultrasonic leak detector was used to determine if a more accurate leak location could be found on the detector. This ultrasonic leak detector functions by detecting a difference in flow by amplifying sounds due to gas movement and reads the signal as sound waves through a headset. The results were a slight increase of gas movement around the outer frame as compared to the background, but it was not located to a specific region. There was no difference around the hex nuts, the window, or the gas plug. The hypothesis that the leak is due to a non-uniform outer frame or non-uniform o-ring stands as the most plausible possibility.

## 4 Noise Reduction Testing

The coaxial cables of the SHV have a grounding cage that have proven in the past to be a source of background noise. This was mitigated by attaching a secondary copper wire to the board ground from the SHV cable's grounding shield. The spark protecting resistors in the past have proven to increase background noise if the legs are left too long. The legs are trimmed down in order to diminish the intensity of the background noise. The high voltage signal from the CAEN power supply goes through a filtering circuit that reduces the noise in the high voltage signal, before sending it to the drift and the well structure of the detector. Placing copper shielding over the detector was avoided in order to assess the performance of the detector without interfering materials.

### 4.1 Quality Control Test Four

The fourth quality control test determines the functionality of the high voltage circuit. The  $\mu$ R-well was not designed with a high voltage circuit and thus this test is rendered unnecessary.

## 5 Current-Voltage Curves

It is important to test the high voltage current of the detector in order to ensure that it is in proper working order. Leakage current on the resistive layer can be indicative of sparking, if a current is seen then sparking is likely to occur. An ideal detector has little to no leakage current, which would imply that no sparking will occur. The leakage current can also alter the potential field created between the top of the wells and the base of the wells. A current-voltage curve is necessary to understand the state of the leakage current. To procure an I-V curve, high voltages are applied in intervals and the current is monitored and recorded. The current achieved by each voltage is then plotted against the corresponding voltage in order to display the relationship. For this test, the large input flow meter was kept stable at 30 units of flow of  $ArCO_2$  and the detector was allowed to sit at an applied voltage on the wells of 100 V prior to testing. An I-V curve was produced for an range up to 600 V.

The time dependence of the leakage current was investigated by taking consecutive measurements, in minute intervals, for each measured voltage. Figure 2 displays the results of this where measurements were taken for one minute intervals spanning a total of five minutes, please note that a few voltages required a span of ten minutes as the current did not stabilize in the five minutes. Four of the applied voltages displayed nonzero currents and are color coded on the graph to the matching curve for the change in current over time. These four points (500 V, 510 V, 520 V, and 530 V) were revisited after the data-taking was completed, and were found to be zero.

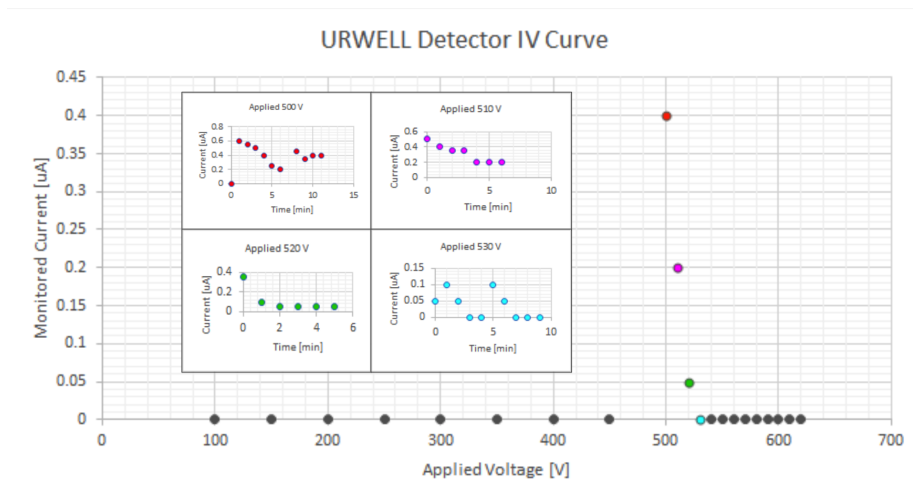


Figure 2: The current vs voltage graph for displaying the leakage current after the detector was allowed to sit for one hour at an applied voltage to the wells of 100 V, for a range of 100 V to 620 V. The non-zero colored points were revisited after the conclusion of the testing and the current was stable at zero.

The results were proven to be reproducible for an applied voltage range of 150 V to 625 V. The large input flow meter was once again kept constant at 30 units of flow and the detector was allowed to sit at an applied voltage to the wells of 100 V for ten minutes. The detector was then kept at each applied voltage for one minute in duration. At each applied voltage the corresponding current was seen to be zero with no spikes or fluctuations, as seen in Figure 3. The high voltage circuit on the  $\mu$ R-well is in ideal working order and the observed leakage current is zero.

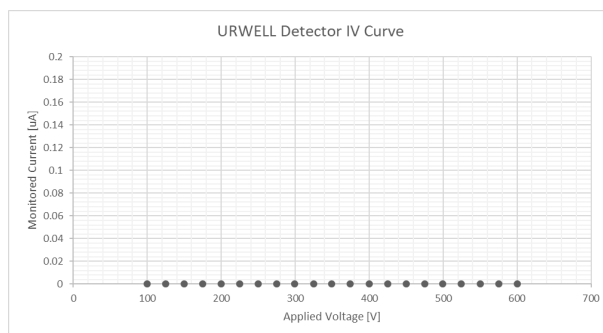


Figure 3: The current vs voltage graph for displaying the leakage current after the detector was allowed to sit for ten minutes at an applied voltage to the wells of 100 V for a range of 100 V to 600 V, confirming there is no leakage current.

## 6 Preamplifier Testing

The laboratory has four preamplifiers, and all four were tested to determine the working condition. Each preamplifier was connected to a waveform generator via the test input, the output of the preamplifier was connected to the oscilloscope. The waveform generator was set to output a Gaussian wave with a 2 volt amplitude and a 4 Hz frequency into each preamplifier. Preamplifier 1 (used for the in-flight setup) showed a 10 V output amplitude and is in working condition. Preamplifier 2 (used for the in-flight setup) showed a 7.5 V output amplitude, however, it is not in working condition. Through later testing it was determined that the input connection on the preamplifier is not working. This was not found while checking the output amplitudes as the waveform generator was not connected to the input of the preamplifier but rather the test input. This preamplifier was originally determined to be in working order, however, it is now documented as a non-functioning preamplifier. Preamplifier 3 (used for the  $\mu$ R-well setup) showed a 2.6 V output amplitude and is in working condition, Figure 4, shows the output signal on the oscilloscope. Preamplifier 4 was labeled as “bad-No signal”, this one was tested in order to confirm the previous labeling. A 2 V input showed no signal output on the oscilloscope and was confirmed to be a non-functioning preamplifier.

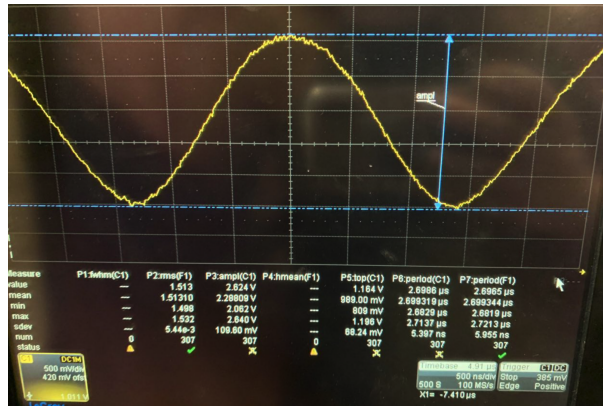


Figure 4: The output signal for Preamplifier 3 when a 2 V, 4 Hz, Gaussian waveform acts as the input. A 2.6 V output amplitude can be seen on the oscilloscope confirming the working status of the preamplifier.

## 7 Conclusion and Future Work

The  $\mu$ R-well has a sturdy design and functions effectively in a harsh radiation environment. The single amplification stage realized by the well structure and the strong honeycomb mounted PCB makes this detector ideal for large area tracking as a larger possible active region means that there will be a smaller dead zone between detectors. Further study will be completed to explore the  $\mu$ R-well and its features that are optimal for the EIC. Quality control test five will be the next step taken where gain curves will be obtained for the assessment of the detector’s performance, as well as direct source testing for the  $\mu$ R-well.